chapter 10

Pulse-Height Spectrometry

Most of the radiation measurement systems used in nuclear medicine use pulse-height analysis (Chapter 8, Section C) to sort out the different radiation energies striking the detector. This is called *pulse-height* or *energy spectrometry.* It is used to discriminate against background radiation, scattered radiation, and so on, and to identify the emission energies of unknown radionuclides. In this chapter we discuss the basic principles of pulse-height spectrometry and some of its characteristics as applied to different types of detectors.

A. BASIC PRINCIPLES

Pulse-height spectrometry is used to examine the amplitudes of signals (electrical current or light) from a radiation detector to determine the energies of radiations striking the detector, or to select for counting only those energies within a desired energy range. This can be accomplished only with those detectors that provide output signals with amplitudes proportional to radiation energy detected, such as proportional counters, scintillation detectors, and semiconductor detectors (Chapter 7). A pulse-height, or energy, *spectrometer* consists of such a radiation detector and its high-voltage supply, preamplifier, amplifier, and pulse-height analyzer (Chapter 8, Section C). A pulse-height *spectrum* is a display showing the number of events detected ("counts") versus the amplitude of those events. This is provided most conveniently by a multichannel analyzer (Chapter 8, Section C.4 and Fig. 8-9).

The spectrum recorded from a radiation source depends not only on the energy of the emissions from the source but also on the type of radiation detector used. It also depends on the mechanisms by which the radiation energy is deposited in the detector. It is important to remember that the amplitude of the signal from a proportional, scintillation, or semiconductor detector depends on the amount of radiation energy *deposited in the detector,* which may be *less* than the full energy of the incident particle or photon.

In the case of particulate radiation (e.g., β particles or α particles), energy is transferred to the detector by collisions with atomic electrons in *primary ionization events.* These electrons may be given sufficient energy to cause *secondary ionizations* in collisions with other atomic electrons (Fig. 10-1A). Approximately 80% of the total ionization from particle-type radiation is the result of secondary ionization. The total amount of ionization produced (primary plus secondary) determines the amplitude of signal out of the detector (electrical current or light). Whether the full energy of the incident particle is deposited in the detector depends primarily on the range of the particle in the detector material. Particle ranges are very short in solids and liquids; thus the energy transfer is complete in most solid and liquid detectors—for example, sodium iodide [NaI(Tl)] and liquid scintillation detectors—and the amplitude of signal from the detector is thus proportional to particle energy. In gas-filled detectors (e.g., proportional counters), however, or in very thin solid detectors (e.g., some semiconductor detectors) that do not have sufficient thickness to stop the particle, the energy transfer may be incomplete. In this case, the amplitude of the signal from the detector will not reflect the total energy of the incident particle.

In the case of photons (γ rays, x rays, bremsstrahlung), energy is transferred to the detector primarily in photoelectric, Compton, or pair-production interactions. A portion of the incident photon energy is transferred as kinetic energy to photoelectrons, Compton electrons, or positive-negative electron pairs,

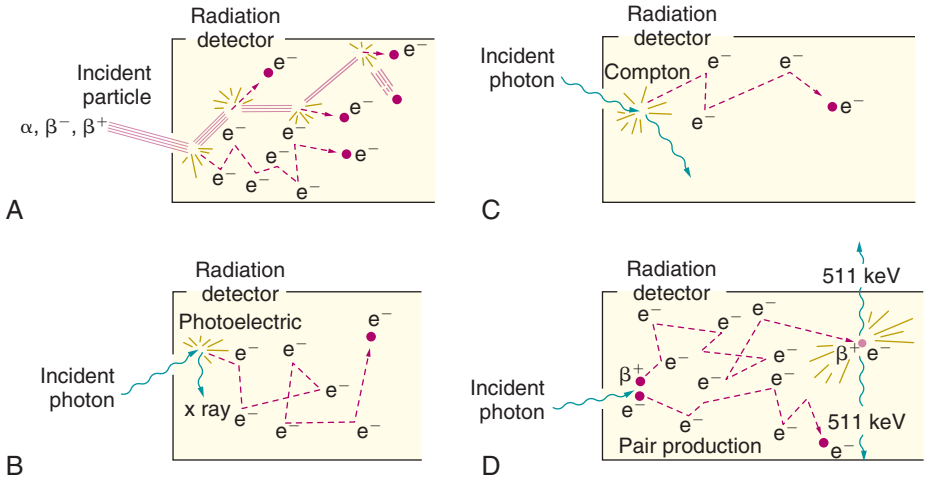

FIGURE 10-1 Deposition of radiation energy in a radiation detector. *A,* Energy transfer from an incident-charged particle to electrons in multiple ionization events. *Filled red circles* indicate electrons generated in primary ionization events and *dashed lines* are their trajectories; other electrons shown are released in secondary ionization events. *B-D,* Energy transfer from incident photon to electrons in photoelectric (*B*), Compton (*C*), and pair-production (*D*) interactions.

respectively, which in turn transfer their kinetic energy to the detector in secondary ionization events (Fig. 10-1B-D). Whether the amplitude of the signal out of the detector reflects the full energy of the incident photon depends on the fate of the remaining energy, which is converted into one or more *secondary photons* (characteristic x ray, Compton-scattered photon, or annihilation photons). A secondary photon may deposit its energy in the detector by additional interactions*; however, if it *escapes* from the detector, then the energy deposited in the detector and the amplitude of the signal from the detector do not reflect the full energy of the incident photon. The amplitude of the signal from the detector reflects only *the amount of energy deposited in it* by the radiation event.

B. SPECTROMETRY WITH NaI(Tl)

Because of its favorable performance-to-cost ratio, a NaI(Tl) scintillator [coupled to a photomultiplier (PM) tube, or in some cases to a photodiode] is the most commonly used detector in nuclear medicine (Chapter 7, Section C). The basic principles of pulse-height spectrometry are illustrated for this detector. Because NaI(Tl) is used almost exclusively for detecting photons (γ rays or x rays, primarily), only photon spectrometry is considered here.

1. The Ideal Pulse-Height Spectrum

Suppose that a monoenergetic γ-ray source is placed in front of a radiation detector. Assume, further, that the energy of the γ rays, E_γ, is less than 1.022 MeV, so that pair-production interactions do not occur. The principle γ-ray interactions with the detector will be by photoelectric absorption and Compton scattering. Most of the photoelectric interactions result in full deposition of the γ-ray energy in the detector (the characteristic x ray usually is also absorbed in the detector). Pulse amplitudes from these events are proportional to E_γ (Fig. 10-2A). With an *ideal* radiation detector, this would produce a single narrow line in the pulse-height spectrum, called the *photopeak*, at a location corresponding to the γ-ray energy E_γ (Fig. 10-2B). In Compton scattering, only a part of the γ-ray energy is transferred to the detector, via the Compton recoil electron. If the scattered γ ray also is absorbed in the detector, the event produces a pulse in the photopeak, whereas if the scattered γ ray escapes, the energy deposited in the detector is less than E_γ. According to Equation 6-14, the energy deposited in the detector in a single Compton scattering event ranges from near zero (small-angle scattering event), up to a maximum value E_{ce}, corresponding to the energy of the recoil electron for 180-degree Compton scattering events

*Note that multiple interactions arising from a single incident photon occur so rapidly in the detector that they appear to be a single event.

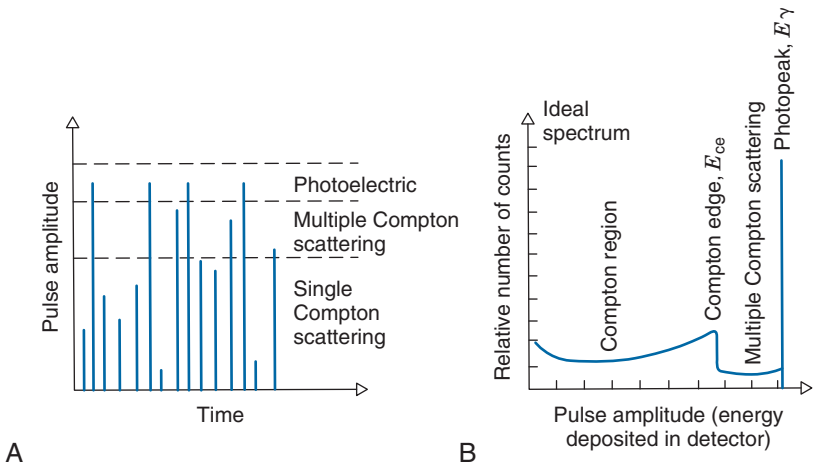

FIGURE 10-2 Elements of an ideal γ-ray pulse-height spectrum. *A,* Pulses from the detector representing different types of γ-ray interactions in the detector. *B,* Distribution (relative number) of pulses versus amplitude (or energy deposited in the detector). Only the photopeak represents deposition of the full energy of the γ ray in the detector.

$$E_{ce} = E_\gamma^2 / (E_\gamma + 0.2555) \qquad (10\text{-}1)$$

where E_γ and E_{ce} are in MeV. The ideal spectrum therefore includes a distribution of pulse amplitudes ranging from nearly zero amplitude up to some maximum amplitude corresponding to the energy given by Equation 10-1. As shown in Figure 10-2B, this part of the spectrum is called the *Compton region.* The sharp edge in the spectrum at E_{ce} is called the *Compton edge.*

Another possibility is that a Compton-scattered γ ray may experience additional Compton-scattering interactions in the detector. Multiple Compton scattering events produce the distribution of pulses with amplitudes in the "valley" between the Compton edge and the photopeak.

2. The Actual Spectrum

In practice, the actual spectrum obtained with a NaI(Tl) spectrometer is quite different from the ideal one shown in Figure 10-2B. For example, Figure 10-3 shows a spectrum obtained from a ^{137}Cs radiation source, which emits 662-keV γ rays and ~30-keV barium x

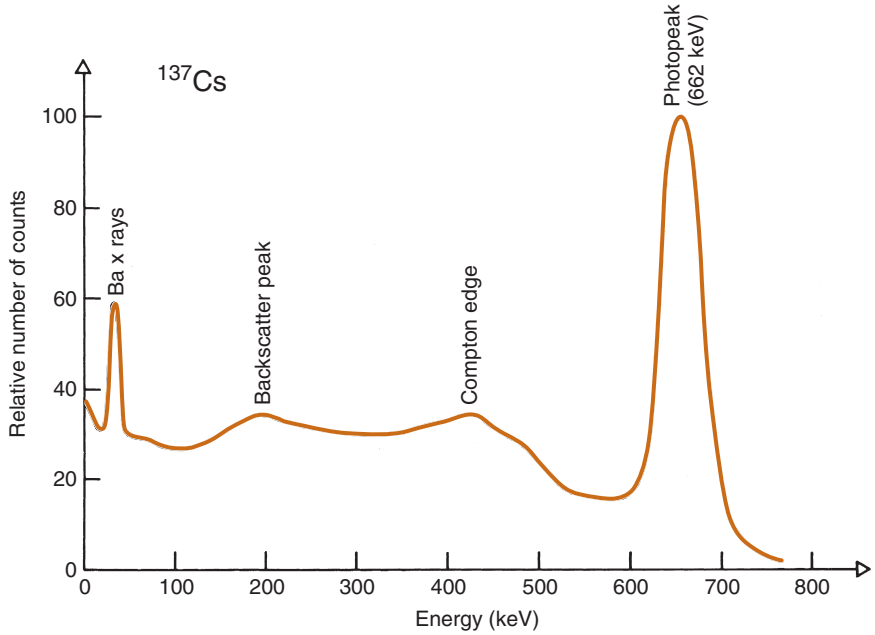

FIGURE 10-3 Actual pulse-height spectrum recorded with a NaI(Tl) detector and ^{137}Cs (662-keV γ rays, ~30 keV Ba x rays). Compare with Figure 10-2B.

rays. The spectrum was recorded with a multichannel analyzer, 0.01 V per channel, with the amplifier gain adjusted so that 662 keV of energy corresponds to 6.62 V of pulse amplitude. Thus the horizontal axis has been translated from pulse amplitude (~0-8 V) into energy (~0-800 keV).

The first feature noted is that the spectrum is "smeared out." The photopeak is not a sharp line, as shown in Figure 10-2B, but a somewhat broadened peak, and the Compton edge is rounded. This is caused by the imperfect energy resolution of the NaI(Tl) detector, discussed in Section B.7.

Another structure that may appear in the spectrum is a *backscatter peak.* This is caused by detection of γ rays that have been scattered toward the detector after undergoing a 180-degree scattering outside the detector. Certain detector configurations enhance the intensity of the backscatter peak. For example, in the well counter (Chapter 12, Section A), a γ ray may pass through the detector without interaction, then scatter back into the detector from the shielding material surrounding it and be detected.

Note that the energy of the backscatter peak, E_b, is the energy of the *scattered* γ ray after 180-degree scattering, whereas the energy of the Compton edge, E_{ce}, is the energy given to the *recoil electron* in a 180-degree scattering event. Therefore

$$E_b + E_{ce} = E_\gamma \qquad (10\text{-}2)$$

Equation 10-2 is helpful for identifying backscatter peaks.

Another structure that may appear is an *iodine escape peak.* This results from photoelectric absorption interactions with iodine atoms in the NaI(Tl) crystal, followed by escape from the detector of the characteristic iodine K-x ray, which has energy of approximately 30 keV. The iodine escape peak occurs at an energy approximately $E_\gamma - 30$ keV; that is, about 30 keV below the photopeak. Iodine escape peaks may be prominent with low-energy γ-ray emitters, for example, ^{197}Hg (Fig. 10-4). Low-energy γ rays are detected by absorption primarily in a thin layer close to the entrance surface of the NaI(Tl) crystal where there is a reasonable probability that the iodine x ray will escape from the detector. With increasing γ-ray energy, the interactions tend to occur deeper within the detector, and there is less likelihood that the x ray will escape. Also, the relative difference between the photopeak and escape peak energies

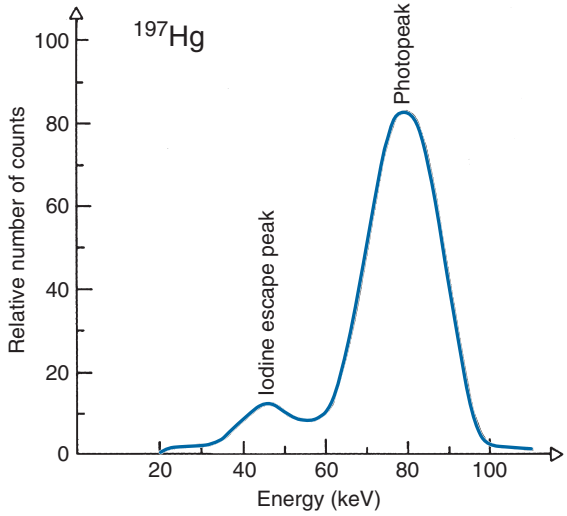

FIGURE 10-4 Pulse-height spectrum for ^{197}Hg (E_γ = 77.3 keV) recorded with NaI(Tl). Iodine escape peak (45-50 keV) is due to escape of characteristic iodine x ray (~30 keV) following a photoelectric absorption event in detector.

becomes smaller, and it becomes more difficult to distinguish between them.

Lead x-ray peaks sometimes are seen in spectra acquired with systems employing lead shielding and collimation. These peaks are caused by photoelectric interactions of the γ rays in the lead. These interactions are followed by emission characteristic 80- to 90-keV lead x rays, which may be recorded by the detector.

If the γ-ray energy exceeds 1.022 MeV, pair production interactions can occur. The kinetic energy given to the positive-negative electron pair is $E_\gamma - 1.022$ MeV (see Chapter 6, Section C.4). In most cases, the entire kinetic energies of both particles are deposited in the detector. When the positron comes to rest, it combines with an electron to create a pair of 511-keV annihilation photons. If both of these photons are absorbed in the detector, the event is recorded in the photopeak. If only one is absorbed, the event is recorded in the *single escape peak,* at energy $E_\gamma - 511$ keV (Fig. 10-5). If both escape, the event is recorded in the double escape peak, at $E_\gamma - 1.022$ MeV.

Scattering within or around the radiation source, or *object scatter,* changes the distribution of radiation energies striking the detector. This is especially important in counting measurements in vivo and in radionuclide imaging because substantial scattering of radiation occurs within the patient. Figure 10-6 shows spectra for ^{131}I with and without scattering material around the source. The

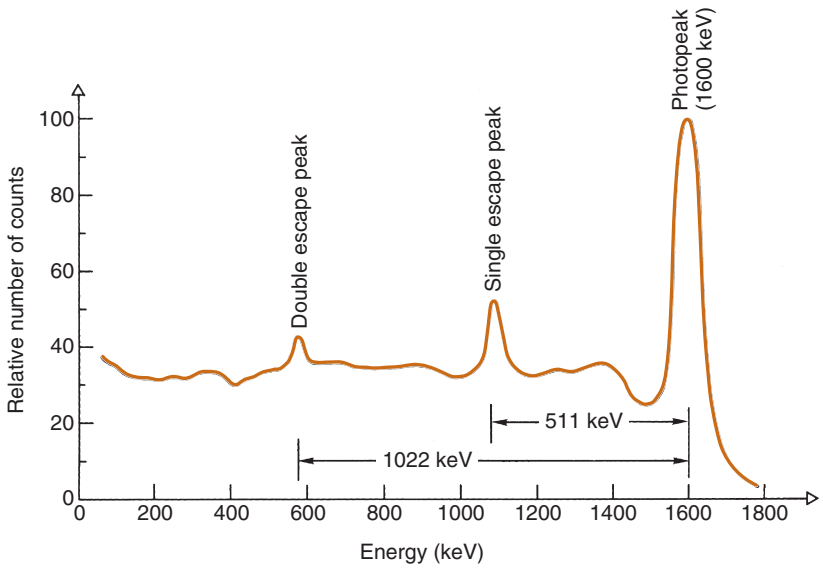

FIGURE 10-5 Pulse-height spectrum for a hypothetical 1.6-MeV (1600-keV) γ-ray emitter. Because γ-ray energy exceeds 1.022 MeV (1022 keV), pair-production interactions can occur in the detector. Escape peaks are due to escape of one or both annihilation photons from the detector following a pair-production interaction.

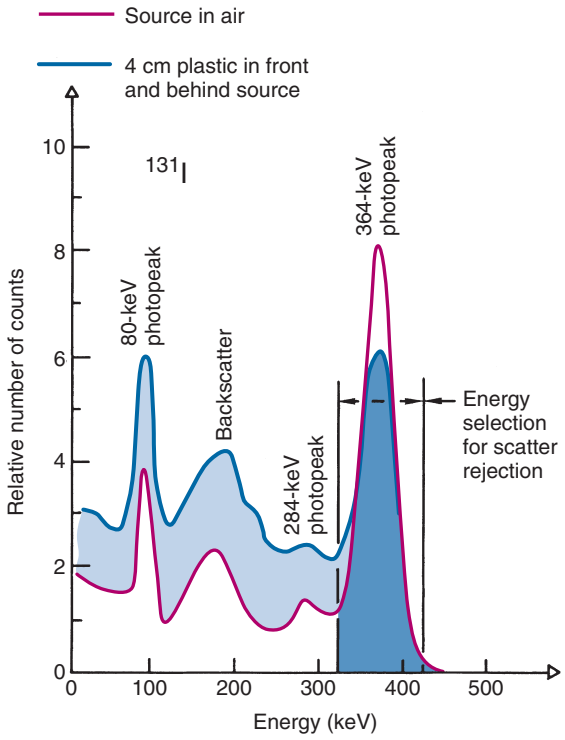

FIGURE 10-6 Effect of scattering material around the source on the pulse-height spectrum for ^{131}I. The *red curve* shows the spectrum with the source in air and the *blue curve* shows the spectrum after placing the source between 4-cm layers of plastic. For the blue curve, the *darker shaded area* represents counts within the photopeak and the *lighter shaded area* represents counts due to γ rays scattered in the plastic.

general effect of object scatter is to add events in the lower-energy region of the spectrum. It is possible to discriminate against scattered radiation by using a pulse-height analyzer to count only events in the photopeak, as shown in Figure 10-6.

Coincidence summing can occur when a radionuclide emits two or more γ rays per nuclear disintegration. Figure 10-7 shows spectra recorded with a NaI(Tl) well counter for ^{111}In, which emits a 173-keV and a 247-keV γ ray simultaneously. The peak at 420 keV seen when the source is inside the well counter results from simultaneous detection of these two γ rays. Summing between x rays and γ rays also can occur. With positron emitters, coincidence summing between the two 511-keV annihilation photons also may be observed. Coincidence summing is especially prominent with detector systems having a high geometric efficiency (see Chapter 11, Section A.2), that is, systems in which there is a high probability that both γ rays will be captured by the detector [e.g., well counters (Chapter 12, Section A)].

3. Effects of Detector Size

The larger the detector crystal size, the more likely it is that secondary photons (i.e., Compton-scattered γ rays and annihilation photons) will be absorbed in the crystal. Thus with increasing crystal size, the number of events in the photopeak versus Compton regions increases. Figure 10-8 shows this

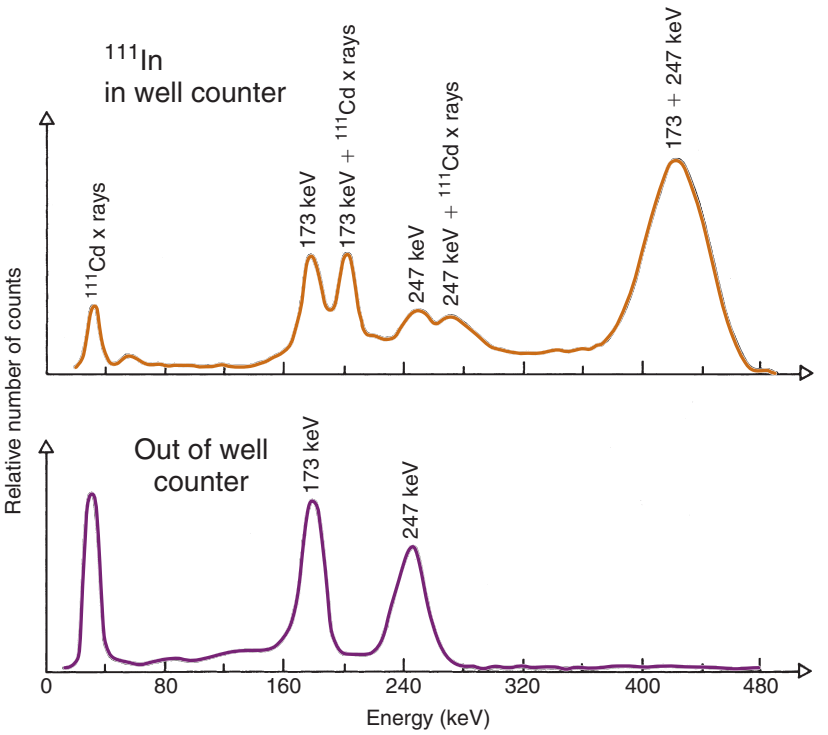

FIGURE 10-7 Pulse-height spectra recorded for ^{111}In with a NaI(Tl) well counter detector. *Top,* Coincidence summing between the x-ray and γ-ray emissions results in additional peaks in the spectrum when the source is inside the well. *Bottom,* When the source is outside the well, the probability of coincidence detection decreases and the coincidence peaks disappear.

effect on the spectrum for ^{137}Cs. Figure 10-8 also shows that the "valley" between the Compton edge and the photopeak at first increases with increasing detector size, due to greater likelihood of an incident photon undergoing multiple Compton interactions within the detector. However, the number of counts in this region eventually decreases due to greater likelihood of complete absorption of the incident photon's energy within the detector, thereby producing an event in the photopeak rather than in the valley. For γ-ray energies greater than 1.022 MeV, the size of annihilation escape peaks also decreases with increasing crystal size.

4. Effects of Counting Rate

Distortions of the spectrum occur at high counting rates as a result of overlap of detector output pulses. Pulse pile-up between two events can produce a single pulse with an amplitude equal to their sum (see Chapter 8, Section B.3). Pile-up between photopeak events and lower-energy events causes a general broadening of the photopeak (Fig. 10-9). This also is one of the causes of dead time losses (see Chapter 11, Section C). There also may be a shift of the photopeak toward lower energies because of baseline shift in the amplifier at high counting rates. Thus if a single-channel analyzer (SCA) is set up at low counting rates on the photopeak and the

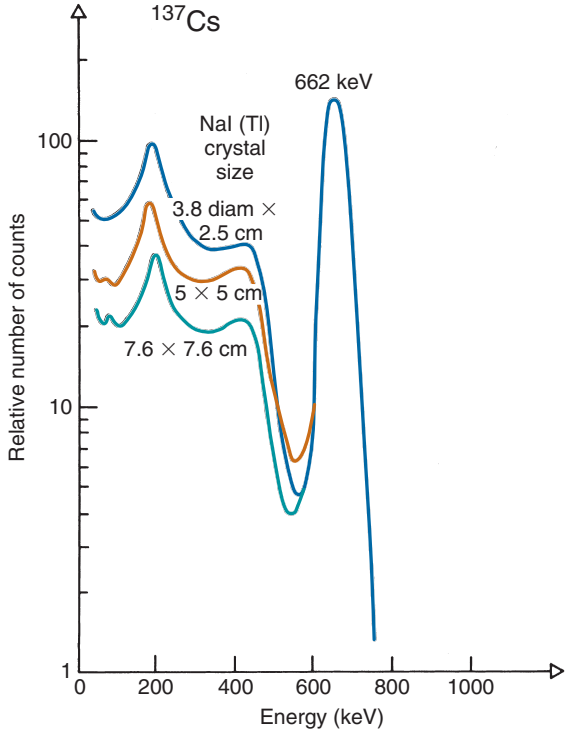

FIGURE 10-8 Effect of NaI(Tl) crystal size on the pulse-height spectrum for ^{137}Cs. The spectra have been normalized to equal photopeak heights. In practice, the photopeak height also increases with increasing detector size because of increasing detection efficiency (Chapter 11, Section A).

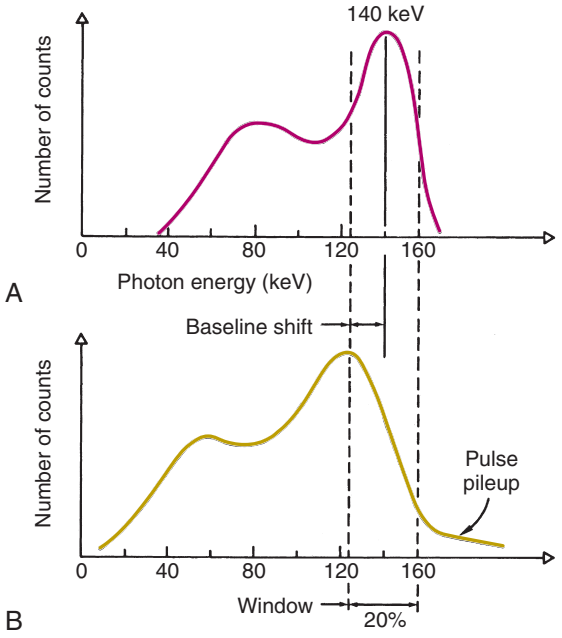

FIGURE 10-9 *A,* ^{99m}Tc spectrum at low counting rate. *B,* Spectral broadening and shift in apparent photopeak energy caused by pulse pileup and baseline shift in the spectrometer amplifier at high counting rate.

detector is used at very high counting rates, the photopeak can shift out of the SCA window and an incorrect reading may be recorded.

5. General Effects of γ-Ray Energy

Figure 10-10 shows pulse-height spectra for a number of radionuclides emitting γ rays of different energies. The solid lines are the spectra for unscattered γ rays, and the dashed lines are the spectra for object-scattered γ rays. In general, the relative number of events in the Compton region versus the photopeak region becomes larger with increasing γ-ray energy because the probability of Compton versus photoelectric interactions in the detector becomes larger. Also, as γ-ray energy increases, it becomes easier to separate object scatter from the photopeak. This is because the change in γ-ray energy with Compton scattering increases with γ-ray energy (see Chapter 6, Section C.3). For example, at 100 keV and at 500 keV, Compton scattering through 90 degrees produces scattered photon energies of 84 keV and 253 keV, respectively. In addition, as discussed in Section B.7 below, the energy resolution of NaI(Tl) detectors improves with increasing γ-ray energy, which provides further improvement in their ability to discriminate between scattered versus unscattered photons.

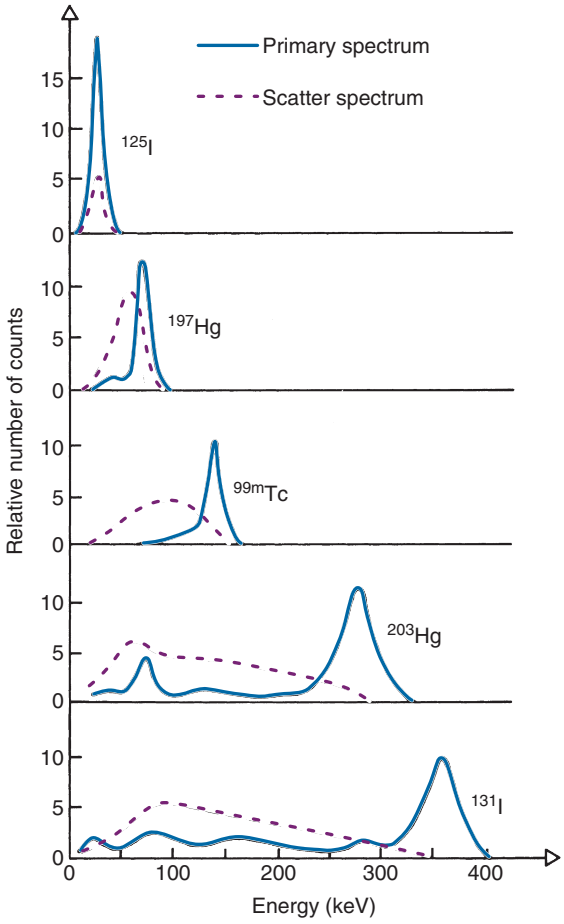

FIGURE 10-10 Pulse-height spectra recorded with a NaI(Tl) detector for different γ-ray energies. *Primary spectrum* refers to γ rays striking the detector without scattering from objects outside the detector. *Scatter spectrum* refers to γ rays that have been scattered by objects outside the detector, such as from tissues or other materials surrounding the source distribution. (*Adapted from Eichling JO, Ter Pogossian MM, Rhoten ALJ: Analysis of scattered radiation encountered in lower energy diagnostic scanning. In Gottschalk A, Beck RN, editors:* Fundamentals of Scanning. *Springfield, IL, 1968, Charles C Thomas.*)

6. Energy Linearity

Energy linearity refers to the proportionality between output pulse amplitude and energy absorbed in the detector. Figure 10-11, taken from early work on the basic properties of NaI(Tl) detectors, shows a typical relationship between apparent energy (pulse height) and actual γ-ray energy for a system calibrated with ^{137}Cs (662 keV). Most NaI(Tl) systems are quite linear for energies between 0.2 and 2 MeV, and a single-source energy calibration usually is acceptable in this range; however, one can run into problems by calibrating a spectrometer with a high-energy source (e.g., ^{137}Cs) and then attempting to use

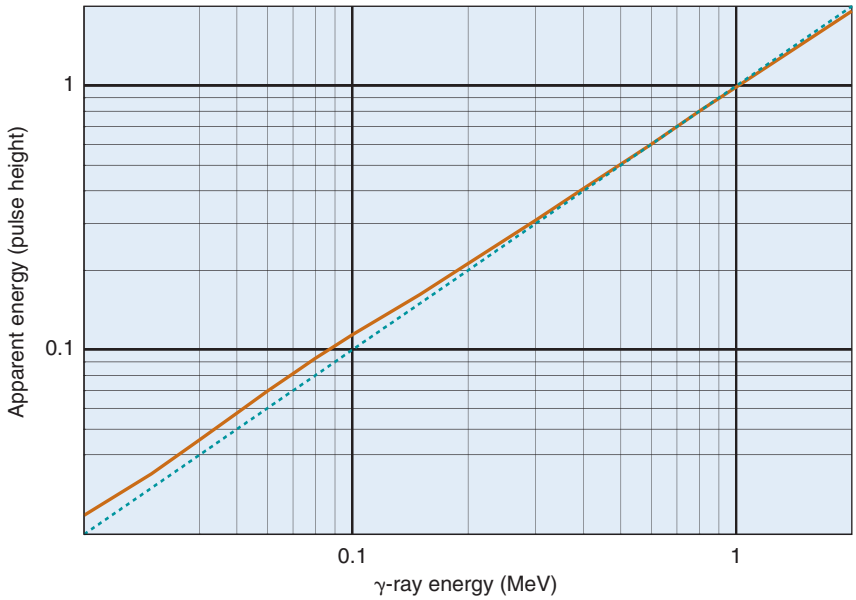

FIGURE 10-11 Apparent energy (pulse height) versus actual γ-ray energy for a NaI(Tl) scintillation detector calibrated for one unit of pulse height per MeV at 0.662 MeV (*solid line*). *Dashed line* is line of identity. With this calibration, detector nonlinearities can lead to 10% to 15% errors in apparent energy for $E_\gamma \lesssim 0.2$ MeV. (*Curve redrawn from Knoll GF:* Radiation Detection and Measurement, *ed 3. New York, 2000, John Wiley, p 339.*)

it for much lower-energy sources (e.g., ^{125}I or ^{99m}Tc) or vice versa. Modern spectrometers and gamma cameras frequently have precalibrated push buttons that are set for specific radionuclides and that take into account any energy nonlinearities. For systems that are not precalibrated, individual low- and high-energy sources should be used to calibrate a spectrometer for measurements that span a wide range of energies.

Energy linearity also is an important factor in energy resolution. This is discussed in the following section.

7. Energy Resolution

Sharp lines and sharp edges in the ideal spectrum (Fig. 10-2B) become broadened lines and rounded edges in actual spectra (Fig. 10-3). With NaI(Tl) detectors, this spectral blurring (or line broadening) is caused primarily by random *statistical variations* in the events leading to the formation of the output signal. For NaI(Tl) coupled to a PM tube, these include the following:

1. Statistical variations in the number of scintillation light protons produced per keV of radiation energy deposited in the crystal
2. Statistical variations in the number of photoelectrons released from the photocathode
3. Statistical variations in the electron multiplication factor of the dynodes in the PM tube

Causes of spectral blurring relating to fabrication of a NaI(Tl) detector assembly include the following:

4. Nonuniform sensitivity to scintillation light over the area of the PM tube cathode
5. Nonuniform light collection efficiency for light emitted from interactions at different locations within the detector crystal

An important but subtle cause of spectral blurring with scintillation detectors is the following:

6. Nonlinear energy response of the scintillator, such that the amount of light produced by the lower-energy Compton electrons in multiple Compton interactions generate a different total amount of light than is produced by a higher-energy photoelectron in a single high-energy photoelectric event, even when the total energy deposited in the crystal is the same (see Section B.6)

Electronic noise contributes to spectral blurring with all types of detectors. With scintillation detectors read out by a PM tube, the principal sources include the following:

7. Fluctuations in the high voltage applied to the PM tube
8. Electrical noise in the PM tube

Because of these factors, there are differences in the amplitude of the signal from a

scintillation detector for events in which precisely the same amount of radiation energy is deposited in the detector. Instead of a narrow "line," the photopeak approximates a gaussian-shaped curve, as illustrated in Figure 10-3. The width of the photopeak, ΔE, measured across its points of half-maximum amplitude is the *energy resolution*. This is referred to as the *full width at half maximum* (FWHM). Usually the FWHM is expressed as a percentage of the photopeak energy E_γ:

$$\text{FWHM}(\%) = (\Delta E/E_\gamma) \times 100\% \qquad (10\text{-}3)$$

Figure 10-12 illustrates this computation. Although FWHM can be computed for any γ-ray energy, it is customary to specify the value for the γ rays of a commonly used radionuclide when characterizing the performance of a particular detector. Examples are the 662-keV γ rays of ^{137}Cs, the 511-keV annihilation photons of positron emitters, or the 140-keV γ rays of ^{99m}Tc. For a gaussian-shaped curve, the FWHM is related to the standard deviation, *SD,* according to

$$\text{FWHM} \approx 2.35 \times SD \qquad (10\text{-}4)$$

For NaI(Tl)-PM tube detectors, a major source of statistical variation in output pulse amplitude is in the number of photoelectrons released from the photocathode of the PM tube. On average, approximately 40 visible light photons are produced per keV of γ-ray energy absorbed in the crystal (see Table 7-2). With good-quality PM tubes and efficient optical coupling, approximately 25% of the light photons yield photoelectrons from the photocathode. Thus the average number of photoelectrons is approximately 10 per keV of radiation energy absorbed in the NaI(Tl) crystal. Complete absorption of a 662-keV γ ray from ^{137}Cs results in the release *on average* of approximately 6600 photoelectrons from the photocathode; however, the actual number varies from one γ ray to the next according to Poisson statistics, with a standard deviation of $\pm\sqrt{6600} \approx 81$ photoelectrons. This amounts to a variation of approximately ±1.2% in pulse amplitude (see Chapter 9, Section B), which translates into an FWHM of approximately 3% (Equation 10-4).

If this were the only source of variation in output pulse amplitude, the energy resolution of NaI(Tl) would be proportional to $1/\sqrt{E}$, because the number of photoelectrons is proportional to the energy deposited in the crystal. However, in practice, the effects of energy are smaller owing to the presence of other sources of pulse amplitude variation. This is evident from a simple comparison of FWHM achievable with a good-quality scintillation detector at 662 keV (about 6%) and the value predicted from simple photoelectron statistics (approximately 3%). The difference is due to other sources of amplitude variations listed earlier. Figure 10-13, showing the observed energy resolution for a NaI(Tl) detector versus a simple $1/\sqrt{E}$ relationship, illustrates this point.

Analyses suggest that photoelectron statistics, PM-tube noise (including electron multiplication), and nonlinear energy response of

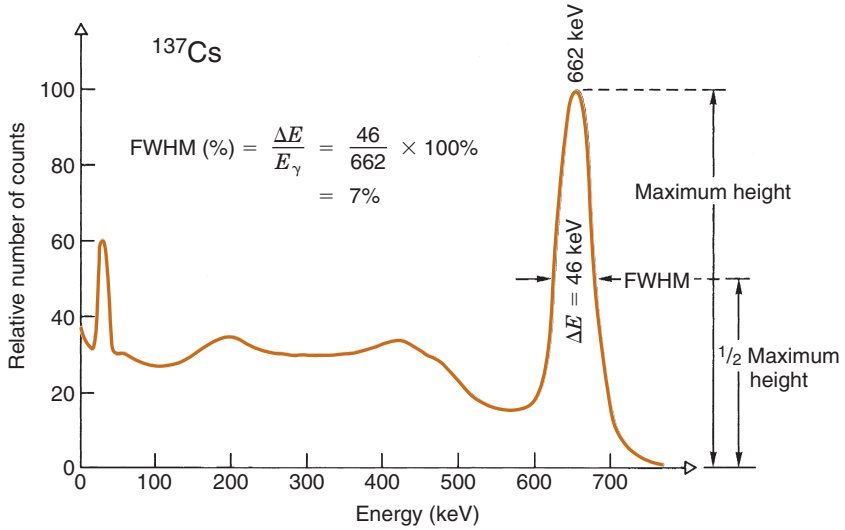

FIGURE 10-12 Calculation of full width at half maximum (FWHM) energy resolution of a NaI(Tl) detector for ^{137}Cs 662-keV γ rays.

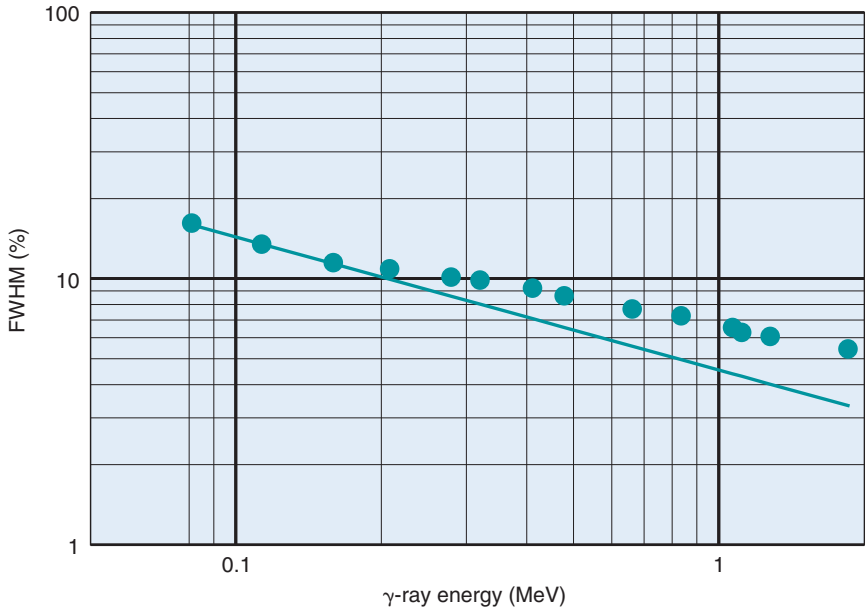

FIGURE 10-13 Energy resolution versus γ-ray energy for a 7.5-cm-diameter × 7.5-cm-thick NaI(Tl) scintillation detector. *Solid line* indicates theoretical $1/\sqrt{E}$ behavior, fitted to low-energy data points. *Experimental data points (●) from Birks JB:* The Theory and Practice of Scintillation Counting. *Oxford, England, 1964, Pergammon Press, p 159.*

the scintillator contribute about equally to overall energy resolution at 662 keV.[1,2] Significant improvements in PM tubes and optical coupling technology have yielded steady improvements in energy resolution during the past 3 to 4 decades. However, the nonlinear energy response of the scintillator may prove to be the limiting factor in achievable energy resolution for NaI(Tl), regardless of further technological improvements. Additional discussions of this complicated issue can be found in reference 1 and other recommended readings at the end of this chapter.

With good-quality PM tubes, energy resolution of 6% at 662 keV is achievable with NaI(Tl). These detectors have energy resolutions of approximately 10% for the 140-keV γ rays of ^{99m}Tc. With large-area crystals having multiple PM tubes [e.g., the gamma camera, (see Chapter 13)], the resolution for ^{99m}Tc can be degraded because of slightly different responses between PM tubes. However, modern gamma cameras employ electronic and software correction schemes to account for these variations and commonly achieve 10% energy resolution for ^{99m}Tc as well (Chapter 14, Section A.3).

Another factor that affects energy resolution is the integration time used to collect signal from the detected event. For routine imaging or spectrometry applications with NaI(Tl), the integration time typically is approximately 1 μsec, in which case the energy resolutions mentioned earlier may be achieved. However, for positron coincidence detection, the integration time may be shortened to only a few hundred nanoseconds to minimize the number of random coincidences between annihilation photons that do not actually arise from the same positron annihilation event (Chapter 18, Section A.9). With shorter integration times, the number of photoelectrons contributing to the detected signal is smaller; hence, energy resolution is degraded. Typically, the energy resolution at 511 keV (the energy of the annihilation photons) may be degraded from a value of 6% to 7% with "full integration" of the detected signal, to a value of approximately 10% with the shortened integration time used in positron coincidence mode.

Other factors that can degrade energy resolution include poor light coupling between the NaI(Tl) crystal and the PM tubes, which can cause a reduction in the number of photoelectrons released per keV. Energy resolution also may be degraded by other conditions that interfere with the efficient collection of light from the crystal by the PM tube. For example, a cracked detector crystal causes internal reflections and trapping of light in the detector crystal. A sudden degradation of

energy resolution and loss of output pulse amplitude often are the first symptoms of a cracked crystal. Deterioration of the optical coupling grease between the detector crystal and PM tube has similar effects. Poor light collection also can occur with detectors having an unusual shape, such as a high aspect ratio (long and narrow).

Good energy resolution is a desirable characteristic for any spectrometer system because it permits precise identification and separation of γ rays with very similar energies, for example, for radionuclide identification or scatter rejection. The best energy resolution is obtained with semiconductor detectors, as discussed in the following section.

C. SPECTROMETRY WITH OTHER DETECTORS

1. Semiconductor Detector Spectrometers

The major advantage of [Si(Li)] and [Ge(Li)] semiconductor detectors (Chapter 7, Section B) is their superb energy resolution. It is typically 6-9 times better than proportional counters and 20-80 times better than NaI(Tl):PM tube detectors. The output signal from a semiconductor detector is a pulse of electrical current, the amplitude of which is proportional to the radiation energy deposited in the detector. The energy resolution of Si(Li) and Ge(Li) detectors is determined by statistical variations in the number of charges in this pulse. The average number is approximately 1 charge (electron) per 3 eV of radiation energy absorbed (see Table 7-1), as compared with only 10 photoelectrons per *keV* in a NaI(Tl):PM tube detector system. The much larger number of charges produced in these semiconductor detectors results in much smaller percentage statistical variations in signal amplitude and hence much better energy resolution than NaI(Tl). Figure 10-14 shows comparative NaI(Tl): PM Table and Ge(Li) spectra for ^{99m}Tc. The superior energy resolution of Ge(Li) permits almost complete elimination of scattered radiation by pulse-height analysis and clean separation of multiple photon emissions from single or multiple sources.

Despite their superior performance in terms of energy resolution, Si(Li) and Ge(Li) detectors have not found widespread usage in nuclear medicine. As explained in Chapter 7, they are available only in relatively small sizes. As well, Ge(Li) must be operated at liquid nitrogen temperatures, which poses practical inconveniences, and Si(Li) detectors are relatively inefficient for the γ-ray energies commonly used in nuclear medicine.

More recently developed "room temperature" semiconductor detectors such as cadmium telluride and cadmium zinc telluride (CZT) (Chapter 7, Section B) may provide more practical options for nuclear medicine. Although their energy resolution is not equal to that of Si(Li) or Ge(Li), owing to somewhat lower production of charge carriers, it is significantly better than NaI(Tl).

Figure 10-15 shows typical pulse-height spectra for ^{99m}Tc and ^{18}F (511-keV annihilation photons) obtained with a CZT detector. A number of interesting features are evident in these spectra. For ^{99m}Tc, the energy resolution is intermediate to that of Ge(Li) and NaI(Tl) (see Fig. 10-14). For both ^{99m}Tc and ^{18}F, there is evidence of a "tail" on the low-energy side of the photopeak. This is caused by "charge trapping" and incomplete charge collection within the CZT crystal. In addition to the main photopeak at 140 keV, a small photopeak is seen at approximately 20 keV. This corresponds to K-x rays of technetium emitted after internal conversion events (~7% emission frequency; see Appendix C). This peak is rarely, if ever, seen in NaI(Tl) spectra owing to attenuation of these x rays by the canning material housing the detector crystal.

The CZT spectrum for ^{18}F shows a well-defined Compton edge (E_{ce} = 341 keV) and backscatter peak (E_b – 170 keV). Also present are peaks at approximately 73 keV and 86 keV, which were caused by characteristic x rays of lead from shielding material placed around the source in this experiment.

Note finally that the energy resolution of the CZT spectra is essentially the same for ^{99m}Tc as for ^{18}F, in spite of a nearly fourfold difference in their γ-ray energies. With NaI(Tl), this would result in a significant difference in energy resolution, owing to a similar difference in the number of photoelectrons emitted by the photocathode of the PM tube. However, with CZT, the equivalent source of line broadening is in the number of charge carriers (electron-hole pairs) produced, which is a significantly larger number. The predominating causes of line broadening with CZT are leakage current through the detector itself and incomplete (and variable) collection of the charge carriers. These factors depend primarily on the operating

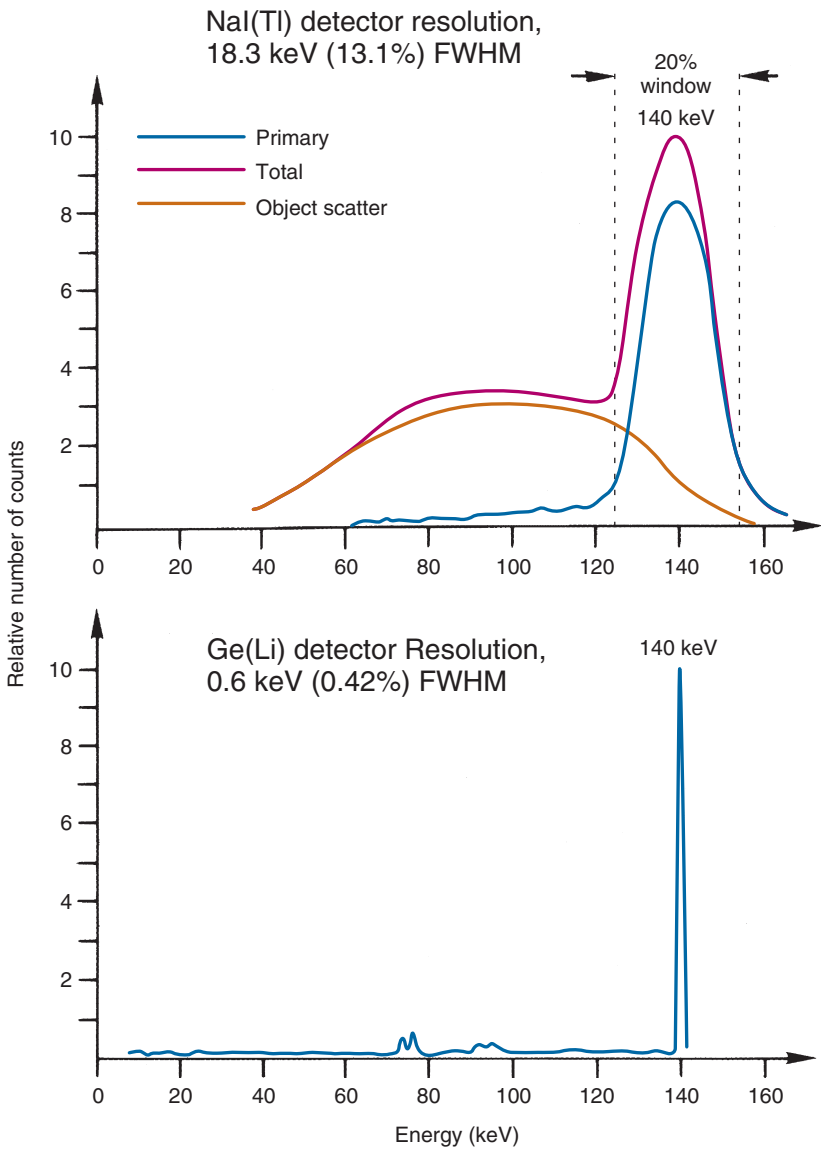

FIGURE 10-14 Comparative pulse-height spectra recorded from a ^{99m}Tc source with NaI(Tl) and Ge(Li) detectors. In the NaI(Tl) spectrum (*top*), the *blue* curve represents unscattered (primary) γ rays, the *orange* curve represents γ rays scattered by materials around the source, and the *red* curve represents the sum of the primary and scattered γ rays. For the Ge(Li) detector (*bottom*), only the spectrum for primary γ rays is shown. Separation of primary from scattered γ rays is much easier with the semiconductor detector.

voltage and on the specific detector configuration (such as electrode attachments). The next most important contributor is electronic noise. None of these factors depend directly on γ-ray energy. Thus the approximate $1/\sqrt{E}$ relationship seen with NaI(Tl) generally does not apply for room-temperature semiconductor detectors.

The performance of CZT detectors can be improved by operating them at low temperatures (thereby reducing background leakage current). This also would at least partially restore a $1/\sqrt{E}$ relationship in their energy resolution; however, this also would eliminate the practical benefits of room-temperature operation.

2. Liquid Scintillation Spectrometry

Although NaI(Tl) spectrometers are used in many different configurations and applications, both for in vivo and in vitro measurements, liquid scintillation spectrometers are used almost exclusively in a single configuration for in vitro sample counting (see Chapter

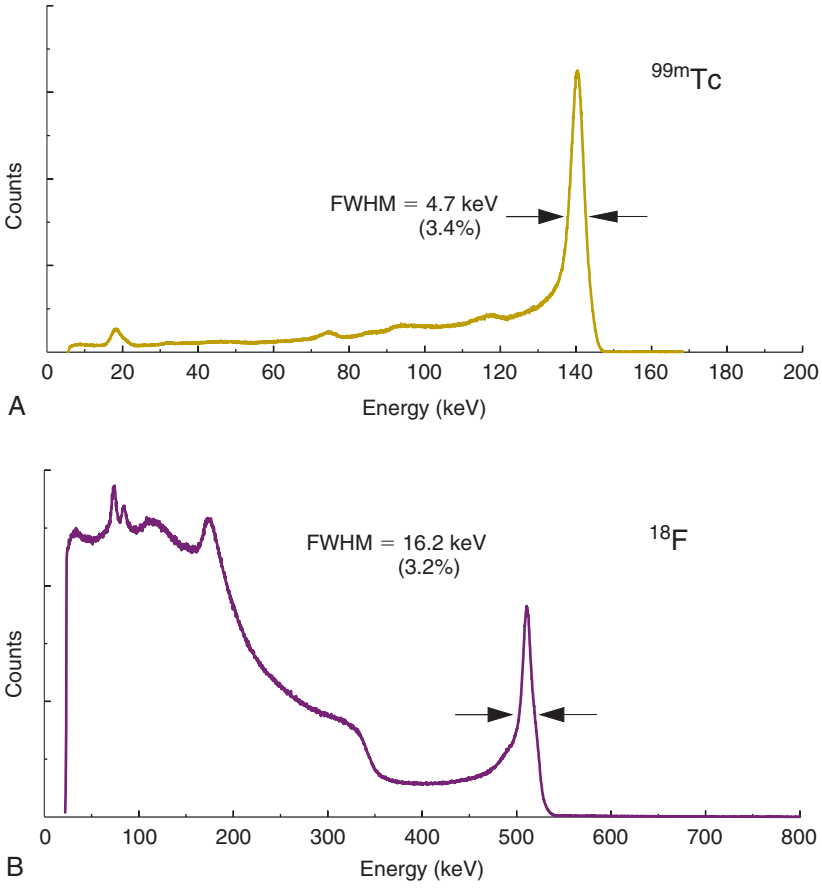

FIGURE 10-15 ^{99m}Tc (*A*) and ^{18}F (*B*) spectra obtained with a 5 × 5 × 5-mm cadmium zinc telluride (CZT) detector, with 0.6-mm-thick Al entrance window and CAPture electrode geometry.[3] The detector was operated at room temperature with an operating voltage of 1000 V for ^{99m}Tc and 1250 V for ^{18}F. FWHM, full width at half maximum. (*Data courtesy Paul Kinahan, University of Washington, Seattle, WA; eV Products, Saxonburg, PA; and James Wear of Lunar Corporation, Madison, WI.*)

12, Section C). Liquid scintillation detectors are used primarily for counting the low-energy β emissions from ^{3}H, ^{14}C, ^{35}S, ^{45}Ca, and ^{32}P.

Figure 10-16 shows pulse-height spectra recorded with a liquid scintillation system for a γ-ray emitter, ^{137}Cs, and for a β emitter, ^{14}C. Liquid scintillators provide poor energy resolution for γ rays because they produce relatively few scintillation light photons per keV of energy absorbed and hence produce relatively few photoelectrons at the PM tube photocathode in comparison with NaI(Tl). Another factor is the relatively inefficient transfer of light photons from the scintillator vial to the PM tubes. The spectrum for a β emitter has no sharp peak because the energy spectrum for β particles has a broad distribution from zero up to E_{β}^{max} for the radionuclide (compare Fig. 10-16 with Fig. 3-2).

3. Proportional Counter Spectrometers

Gas-filled proportional counters (Chapter 7, Section A.3) have found limited use for spectrometry in nuclear medicine. Their energy resolution is several times better than NaI(Tl).

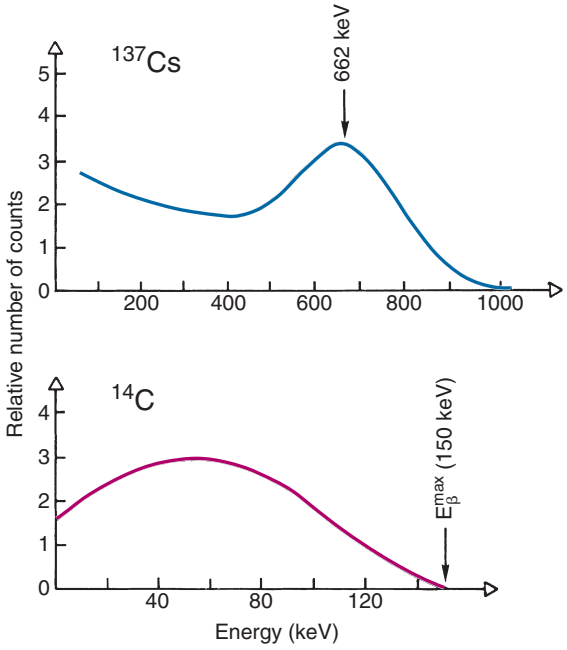

FIGURE 10-16 Pulse-height spectra recorded with a liquid scintillation detector, for a γ-ray emitter, ^{137}Cs (*top*), and a β emitter, ^{14}C (*bottom*).

Their major disadvantage is poor detection efficiency for γ rays (see Chapter 11, Section A.3). Some applications of proportional counter spectrometry are discussed in Chapter 12.

REFERENCES

1. Dorenbos P, de Haas JTM, van Eijk CWE: Non-proportionality of scintillation response and the energy resolution obtainable with scintillation crystals. *IEEE Trans Nucl Sci* 42:2190-2202, 1995.
2. Valentine JD, Rooney BD, Li J: The light yield non-proportionality component of scintillator energy resolution. *IEEE Trans Nucl Sci* 45:512-517, 1998.
3. Parnham K, Szeles C, Lynn KG, Tjossem R: Performance improvement of CdZnTe detectors using modified two-terminal electrode geometry. *SPIE Conference on Hard X-Ray, Gamma-Ray and Neutron Detector Physics*, Denver, CO, July 1999.

BIBLIOGRAPHY

Additional discussion of NaI(Tl) pulse-height spectrometry may be found in the following:

Birks JB: *The Theory and Practice of Scintillation Counting*, New York, 1964, MacMillan.

Hine GJ: Sodium iodide scintillators. In Hine GJ, editor: *Instrumentation in Nuclear Medicine*, Vol 1, New York, 1967, Academic Press, Chapter 6.

Spectrometry with Si(Li) and Ge(Li) semiconductor detectors is discussed in the following:

TerPogossian MM, Phelps ME: Semiconductor detector systems. *Semin Nucl Med* 3:343-365, 1973.

Spectrometry with room-temperature semiconductor detectors is discussed in the following:

Schlesinger TE, James RB, editors: Semiconductors for room temperature nuclear detector applications. In *Semiconductors and Semimetals*, Vol 43, San Diego, 1995, Academic Press. (Chapters 8, 9, and 14 are of particular interest.)

A useful general reference for pulse-height spectrometry is the following:

Knoll GF: *Radiation Detection and Measurement*, ed 4, New York, 2010, John Wiley.